Hydrological Sciences Journal
Publication details, including instructions for authors and subscription information:
http://www.tandfonline.com/loi/thsj20

Rainfall-interception-evaporation-runoff relationships in a semi-arid catchment, northern Limpopo basin, Zimbabwe

David Love [a b], Stefan Uhlenbrook [c d], Gerald Corzo-Perez [e], Steve Twomlow [f] & Pieter van der Zaag [c d]

[a] WaterNet, PO Box MP600, Mount Pleasant, Harare, Zimbabwe
[b] ICRISAT Bulawayo, Matopos Research Station, PO Box 776, Bulawayo, Zimbabwe
[c] UNESCO-IHE, Westvest 7, PO Box 3015, 2601, DA Delft, The Netherlands
[d] Department of Water Resources, Delft University of Technology, PO Box 5048, 2600, GA Delft, The Netherlands
[e] Hydrology and Quantitative Water Management Group, Centre for Water and Climate, Wageningen University, Droevendaalsesteeg, 4, 6708, PB Wageningen, The Netherlands
[f] United Nations Environmental Programme, PO Box 30552 (00100), Nairobi, Kenya

Published online: 05 Jul 2010.

Rainfall–interception–evaporation–runoff relationships in a semi-arid catchment, northern Limpopo basin, Zimbabwe

David Love[1,2], Stefan Uhlenbrook[3,4], Gerald Corzo-Perez[5], Steve Twomlow[6] & Pieter van der Zaag[3,4]

[1]*WaterNet, PO Box MP600, Mount Pleasant, Harare, Zimbabwe*
dlove@waternetonline.org; baba.kathy@yahoo.com

[2]*ICRISAT Bulawayo, Matopos Research Station, PO Box 776 Bulawayo, Zimbabwe*

[3]*UNESCO-IHE, Westvest 7, PO Box 3015, 2601 DA Delft, The Netherlands*

[4]*Department of Water Resources, Delft University of Technology, PO Box 5048, 2600 GA Delft, The Netherlands*

[5]*Hydrology and Quantitative Water Management Group, Centre for Water and Climate, Wageningen University, Droevendaalsesteeg 4, 6708 PB Wageningen, The Netherlands*

[6]*United Nations Environmental Programme, PO Box 30552 (00100), Nairobi, Kenya*

Received 17 February 2009; accepted 31 March 2010; open for discussion until 1 January 2011

Citation Love, D., Uhlenbrook, S., Corzo-Perez, G., Twomlow, S. & van der Zaag, P. (2010) Rainfall–interception–evaporation–runoff relationships in a semi-arid catchment, northern Limpopo basin, Zimbabwe. *Hydrol. Sci. J.* **55**(5), 687–703.

Abstract Characterizing the response of a catchment to rainfall, in terms of the production of runoff *vs* the interception, transpiration and evaporation of water, is the first important step in understanding water resource availability in a catchment. This is particularly important in small semi-arid catchments, where a few intense rainfall events may generate much of the season's runoff. The ephemeral Zhulube catchment (30 km^2) in the northern Limpopo basin was instrumented and modelled in order to elucidate the dominant hydrological processes. Discharge events were disconnected, with short recession curves, probably caused by the shallow soils in the Tshazi sub-catchment, which dry out rapidly, and the presence of a dambo in the Gobalidanke sub-catchment. Two different flow event types were observed, with the larger floods showing longer recessions being associated with higher (antecedent) precipitation. The differences could be related to: (a) intensity of rainfall, or (b) different soil conditions. Interception is an important process in the water balance of the catchment, accounting for an estimated 32% of rainfall in the 2007/08 season, but as much as 56% in the drier 2006/07 season. An extended version of the HBV model was developed (designated HBVx), introducing an interception storage and with all routines run in semi-distributed mode. After extensive manual calibration, the HBVx simulation satisfactorily showed the disconnected nature of the flows. The generally low Nash-Sutcliffe coefficients can be explained by the model failing to simulate the two different observed flow types differently. The importance of incorporating interception into rainfall–runoff is demonstrated by the substantial improvement in objective function values obtained. This exceeds the gains made by changing from lumped to semi-distributed mode, supported by 1 000 000 Monte Carlo simulations. There was also an important improvement in the daily volume error. The best simulation, supported by field observations in the Gobalidanke sub-catchment, suggested that discharge was driven mainly by flow from saturation overland flow. Hortonian overland flow, as interpreted from field observations in the Tshazi sub-catchment, was not simulated so well. A limitation of the model is its inability to address temporal variability in soil characteristics and more complex runoff generation processes. The model suggests episodic groundwater recharge with annual recharge of 100 mm year^{-1}, which is similar to that reported by other studies in Zimbabwe.

Key words HBV; interception; Limpopo basin; semi-arid hydrology

Relations précipitation–interception–évaporation–écoulement dans un bassin versant semi-aride (nord du Limpopo, Zimbabwe)

Résumé La caractérisation de la réponse d'un bassin versant aux précipitations, en termes de production d'écoulement par rapport à l'interception, la transpiration et l'évaporation, est un premier pas important pour la compréhension de la disponibilité des ressources en eau dans un bassin. Ceci est particulièrement important dans un petit bassin semi-aride où quelques événements pluvieux intenses peuvent générer l'essentiel de l'écoulement pour la saison. Le bassin versant éphémère Zhulube (30 km^2) dans le nord du Limpopo a été équipé et modélisé de façon à identifier le processus hydrologique dominant. Les épisodes d'écoulement sont déconnectés, avec des courbes de récession courtes, probablement dues aux horizons peu épais du sous-bassin Tshazi, qui sèchent rapidement, et à la

ISSN 0262-6667 print/ISSN 2150-3435 online

doi: 10.1080/02626667.2010.494010
http://www.informaworld.com

présence d'un bas-fond dans le sous-bassin Gobalidanke. Deux types différents d'épisodes d'écoulement ont été observés, les crues les plus fortes ayant des récessions plus longues associées à des précipitations (antécédentes) plus élevées. Les différences peuvent être associées à: (a) l'intensité des précipitations, ou (b) différents états des sols. L'interception est un processus important pour le bilan hydrologique du bassin, représentant 32% (estimés) des pluies de la saison 2007/08, et jusqu'à 56% durant la saison plus sèche 2006/07. Une version étendue du modèle HBV a été développée (appelée HBVx) introduisant un stockage par interception, dont toutes les routines opèrent en mode semi-distribué. Après un calage manuel poussé, la simulation HBVx a montré de façon satisfaisante la nature déconnectée des écoulements. Les coefficients de Nash-Sutcliffe généralement bas peuvent être expliqués par l'échec du modèle à simuler différemment les deux types distincts d'écoulement observés. L'importance d'incorporer l'interception dans le modèle pluie-débit est démontrée par l'amélioration substantielle des valeurs obtenues de la fonction objectif. Ceci apporte plus que de passer d'un mode global à semi-distribué, supporté par 1 000 000 simulations de type Monte Carlo. Il y a aussi une amélioration importante de l'erreur du volume journalier. La meilleure simulation, supportée par les observations de terrain dans le sous-bassin Gobalidanke, suggère que le débit est surtout contrôlé par les écoulements de surface dus à la saturation. L'écoulement hortonien, interprété à partir des observations de terrain dans le sous-bassin Tshazi, n'a pas été aussi bien simulé. Une limitation du modèle est son incapacité à représenter la variabilité temporelle des caractéristiques des sols et des processus plus complexes de génération du ruissellement. Le modèle suggère une recharge souterraine épisodique avec une recharge annuelle de 100 mm an^{-1}, ce qui est similaire à ce qui a été rapporté dans d'autres études.

Mots clefs HBV; interception; bassin du Limpopo; hydrologie en milieu semi-aride

INTRODUCTION

Characterizing the response of a catchment to rainfall, in terms of the production of runoff *vs* the interception, transpiration and evaporation of water, is the first step in understanding water resource availability in a catchment. This is particularly important in semi-arid catchments, where a few intense rainfall events may generate much, or sometimes most, of the season's runoff (e.g. Lange & Leinbundgut, 2003) and where spatial and temporal variability of rainfall can be high (e.g. Unganai & Mason, 2002). An understanding of the hydrological processes involved in a catchment is a basic requirement for integrated water resources management planning (e.g. Uhlenbrook *et al.*, 2004). In southern Africa, where environmental and water stress is increasing (Nyabeze, 2004; Sivakumar *et al.*, 2005), this type of understanding is essential in building resilience to large or catastrophic environmental changes and in developing trade-offs between food and economic production and ecosystem services (Falkenmark *et al.*, 2007). It is also important for addressing broader humanitarian and development needs, through the many water intensive interventions that have been proposed by development agencies and projects (Love *et al.*, 2006).

For meso-catchments (scale of approximately 10^1–10^3 km^2; Blöschl & Sivapalan, 1995), internal heterogeneities are very important (Didszun & Uhlenbrook, 2008). Evaporation processes, including interception, play a controlling role in runoff generation (Bullock, 1992), and interception is a major driver of the magnitude and speed of catchment response to rainfall, especially for semi-arid catchments with limited rainfall frequency and depth, and especially for smaller storm events (Seyam *et al.*, 2000; Smith & Rethman, 2000; Beven, 2002; De Groen & Savenije, 2006; Tsiko *et al.*, 2008). Despite this, many modelling studies either ignore interception, or consider it part of a lumped evaporation parameter (e.g. Smith & Rethman, 2000).

For semi-arid catchments, properties such as soil depth and permeability are also important, with percolation beginning much faster in catchments with shallower soil profiles (Chesson *et al.*, 2004). Shallower soils dry more rapidly, which can reduce connectivity between discharge events (Farmer *et al.*, 2003), although in seasonal wetlands the narrow profile above an impermeable clay layer may remain saturated throughout the rainy season (McCartney *et al.*, 1998). During high-intensity rainfall, a soil's infiltration capacity can be rapidly reached, leading to overland flow as the initial phase of surface runoff. This process has been shown to become more dominant with increasing aridity in a number of study sites (Lange & Leinbundgut, 2003) and increasing land degradation (Martinez-Mena *et al.*, 1998). This emphasises the importance of differences in soil properties and land cover.

In data-poor regions, with ongoing declines in hydrological networks, hydrological prediction remains a challenge (Sivapalan *et al.*, 2003). Where networks can be improved or extended, this is of course valuable – even a small number of discharge measurements can improve our understanding of a catchment or the performance of a model (Seibert & Beven, 2009). Such observations can be used to improve our understanding of the scientific basis of hydrology and of catchment response, which is a fundamental requirement for predictions in ungauged basins, one of the oldest and most critical tasks in hydrology – which has received increasing prominence under the International Association of Hydrological Scientists' PUB (Prediction in Ungauged Basins) initiative.

In this study, the response to rainfall of a meso-catchment in the semi-arid northern Limpopo basin is studied and modelled. This is the first attempt at process-based hydrological modelling in the trans-boundary northern Limpopo basin – although such studies have been carried out in headwater catchments of the Save and Zambezi basins (e.g. McCartney *et al.*, 1998; Mugabe *et al.*, 2007). The objective of the study was to elucidate the dominant hydrological processes in the catchment. A dynamic, semi-distributed model was developed to analyse the rainfall–interception–evaporation–runoff relationships.

METHODS

Study area

The northern Limpopo basin in Zimbabwe is a semi-arid area, with rainfall varying from 360 mm year^{-1} in the south to 630 mm year^{-1} in the north (Love *et al.*, 2010). Rainfall is seasonal, controlled by the Inter Tropical Convergence Zone and falling between October–November and March–April (Makarau & Jury, 1997). Rainfall occurs over a limited period of time, and often a large portion of the annual rainfall can fall in a small number of events (De Groen & Savenije, 2006). The selected study catchment, Zhulube, is a tributary of the upper Mzingwane River, located 87 km south-east of Bulawayo, Zimbabwe (Fig. 1). Mean annual rainfall for the nearest climate station (Filabusi, 4 km from the northern edge of the catchment) was 555 mm year^{-1} for the period 1921–2006. The catchment is covered mainly by mixed *Hyparrehenia* grassland and *Bracyhstegia* woodland, with highveld forest prominent in the northern Tshazi sub-catchment (23 km^2) and degraded land prominent in the southern Gobalidanke sub-catchment (7 km^2). Rainfed fields occupy the downstream portion of the catchment (Fig. 1). The Tshazi sub-catchment consists of steep, forested hills (altitude 1000–1200 m a.m.s.l.; slope 3–20%), with thin, rocky lixisols, whilst the Gobalidanke sub-catchment is a shallow valley (altitude 1000 m a.m.s.l.; slope 1.3%) between granite inselbergs (altitude 1000–1100 m a.m.s.l.; slope 4–12%), underlain by luvisols (Fig. 2). The centre of the valley is a dambo, defined as a grass-covered, treeless seasonal wetland on hydromorphic soils (Wright, 1992), with a thin sandy horizon above a clay layer, superimposed on deeper sandy soil (Von der Hayden & New, 2003). Dambos are common in head-water streams on the Zimbabwean highveld (McCartney *et al.*, 1998). The Tshazi sub-catchment has eight

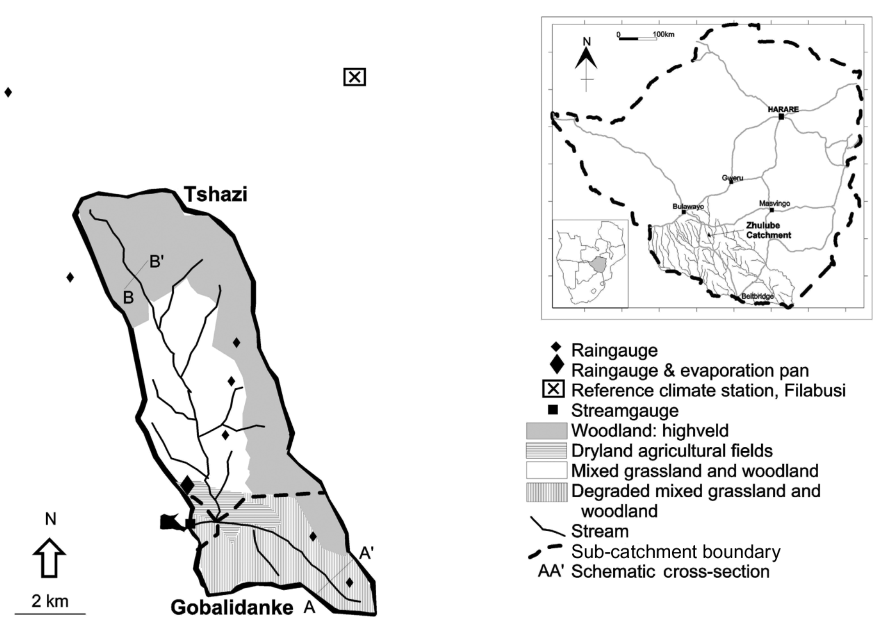

Fig. 1 The Zhulube catchment, showing sub-catchments, land cover, instrumentation and location of reference climate stations. Land cover was derived from a false colour composite using bands 3, 4 and 5 from Landsat scene p170r074, supported by ground truthing. Inset: location in Zimbabwe.

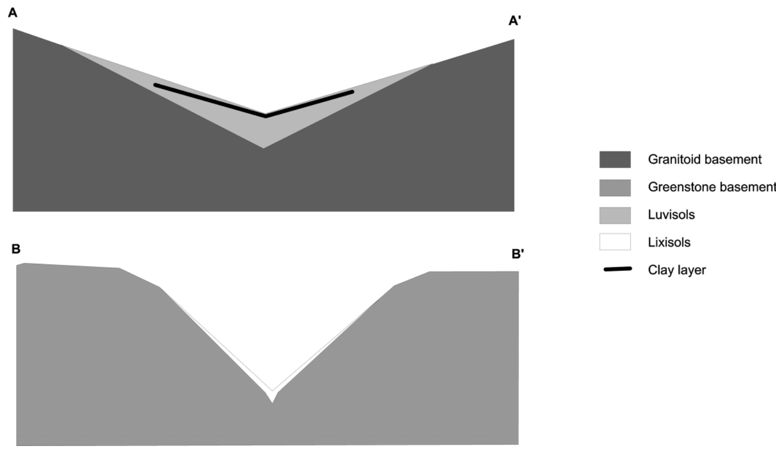

Fig. 2 Schematic cross-sections through the Zhulube catchment, based on geological mapping by Tunhuma *et al.* (2007), and field observations in gullies and artisanal mine workings. AA′ is in the Gobalidanke sub-catchment and BB′ in the Tshazi sub-catchment. Not to scale.

tributaries with catchment areas over 1 km^2, whilst the Gobalidanke sub-catchment has four. Tributaries in both sub-catchments only flow during and immediately after some storm events.

Field data

The catchment was instrumented with rainfall catch-gauges as shown in Fig. 1. These were read daily, and daily rainfall for each sub-catchment was computed by use of Thiessen polygons, from the 2005/06 rainy season onwards. All eight gauges were available for the 2007/08 rainy season, but only five for the 2006/07 season and four for 2005/06. A composite gauge (V notch and broad crest) was constructed at the catchment outlet in December 2006 and readings were taken daily at 08:00 and 16:00 h, with some additional readings taken manually during large storms. The latter procedure was instituted due to the repeated failures of auto-logging pressure transducers and the remote location of the gauge: the field assistant reported to the gauge during large storms and recorded the discharge level every ten minutes. Quality control of observations was made. A theoretical rating equation was used.

A daily antecedent precipitation index was determined for the time series, after the method of Casenave & Valentin (1992):

$$\mathrm{API}i = (\mathrm{API}_{i-1} + P_{i-1})\mathrm{e}^{-\alpha t} \quad (1)$$

where API_i is the antecedent precipitation index for day i (mm d^{-1}), P_i is the rainfall recorded for day i (mm d^{-1}), α is a weight, assigned the value of 0.5 as widely used in semi-arid regions, and t is the time which has elapsed since the last rainfall event prior to day i.

From this a daily antecedent effective precipitation index was determined by replacing rainfall in equation (1) with rainfall less interception (estimated according to equation (7) below).

Multiple regression rainfall–runoff model

A spreadsheet-based multiple regression model was prepared to study the rainfall–runoff relationships in the Zhulube catchment. The model generated effective rainfall and simulated runoff through multiple linear regression for different interception thresholds and by considering different number of days of antecedent rainfall. In addition to other observations, the model was used to calibrate the interception threshold D, which determines the maximum amount of water that can be stored on the land and vegetation surface (Seyam *et al.*, 2000; De Groen & Savenije, 2006).

Estimation of interception and evaporation

Daily reference evaporation was calculated using the Hargreaves formula (equation (2); Allen *et al.*, 1998). It has been suggested that this formula, which is based on temperature and radiation, provides the best input for streamflow simulations in semi-arid areas (Oudin *et al.*, 2005):

$$E_0 = 0.0023(T_{\text{mean}} + 17.8)(T_{\text{max}} - T_{\text{min}})^{0.5}(0.408\text{Ra}) \quad (2)$$

where E_0 is reference evapotranspiration (mm d^{-1}) incorporating interception evaporation, transpiration and soil evaporation, T_{mean} is mean daily temperature (°C), T_{max} is maximum daily temperature (°C), T_{min} is minimum daily temperature (°C) and Ra is daily insolation (J m^{-2} d^{-1} × 10^6). Temperature and radiation data were taken from the West Nicholson climate station, which was the closest station with such data (48 km from the study site).

Potential evapotranspiration for different land covers was derived using:

$$E_i = \text{Kc}_i \, E_0 \quad (3)$$

where E_i is the potential evapotranspiration for land cover i (mm d^{-1}) and Kc$_i$ is the crop coefficient for land cover i (-). The crop coefficient selected for maize varies according to the stage of development; values from Allen *et al.* (1998) and FAO (2010) for East Africa were used. For other land covers, South African equivalents were selected, varying monthly (Table 1).

From these data and the mapped land-cover distribution (Fig. 1), potential evapotranspiration at sub-catchment level was calculated:

$$E_c = X_1E_1 + X_2E_2 + \ldots + X_nE_n \quad (4)$$

where E_c is the potential evapotranspiration at sub-catchment level (mm d^{-1}) and X_i is the area fraction of the sub-catchment under land cover i (-).

Since interception is a threshold process (Seyam *et al.*, 2000; Savenije, 2004; Fenicia *et al.*, 2008), daily interception can be calculated using:

$$I_i = \min(P_i, D) \quad (5)$$

where I_i is the interception for day i (mm d^{-1}), P_i is the rainfall recorded for day i (mm d^{-1}) and D is the interception threshold (mm d^{-1}) (Savenije, 2004). However, if some rainfall was intercepted on the previous day, and the amount of rainfall intercepted was more than could be evaporated on that day, some moisture would remain in interception storage until the next day, thus decreasing the available volume of interception storage for that day. It is assumed that moisture in interception storage at sub-catchments level evaporates with reference to potential evapotranspiration (E_c). A daily interception time series was thus determined for each sub-catchment:

$$S_i = \max(I_i - E_{ci}, 0) \quad (6)$$

$$I_i = \min(P_i, D - S_{i-1}) \quad (7)$$

where S_i is the stored interception at the end of day i (mm) and E_{ci} is the potential evaporation at sub-catchment level on day i (mm d^{-1}). Equation (7) could also be extended to consider interception storage carried from more than one day antecedent.

Daily interception values (from equation (7)) were then used to derive daily transpiration and soil evaporation, which were not further separated:

$$E_{sc} + T_c = \max(E_c - I_i, 0) \quad (8)$$

where E_{sc} is soil evaporation (mm d^{-1}) and T_c is net transpiration (mm d^{-1}), both for the weighted land covers as combined in equation (4), at sub-catchment level as indicated by the subscript c.

The HBVx model and model application

The HBV (Hydrologiska Byråns Vattenbalansmodell) family of models, whilst developed and applied

Table 1 Crop coefficients used for different land cover types, varying by season.

Land cover, this study	South African equivalent	Jan	Feb	Mar	Apr	May	Jun	Jul	Aug	Sep	Oct	Nov	Dec
Woodland: highveld	Woodland (indigenous tree/bush savanna)[a]	1.14	1.14	1.14	1.14	1.00	1.00	1.00	1.00	1.07	1.14	1.14	1.14
Mixed grassland and woodland	Mixed bushveld[b]	1.00	1.00	0.93	0.86	0.71	0.64	0.57	0.64	0.79	0.93	0.93	1.00
Mixed grassland and woodland (degraded)	Veld in poor condition[c]	0.79	0.79	0.79	0.64	0.29	0.29	0.29	0.29	0.43	0.57	0.71	0.79

Source: [a]Jewitt (1992), [b]Schulze & Hols (1993), and [c]Schulze *et al.* (1995). The original crop coefficients were derived for use with pan evaporation data (Schulze *et al.*, 1995). These were converted for use with reference evapotranspiration data by dividing the original crop coefficient with the pan coefficient (taken as 0.7).
Note: For distribution of the land cover types, see Fig. 1.

initially in Sweden, have also been used in semi-arid and arid countries such as Australia and Iran (Oudin *et al.*, 2005; Masih *et al.*, 2008). The application of HBV in Zimbabwe has previously been limited to the humid subtropical climate of eastern and northern Zimbabwe (Lidén & Harlin, 2000).

The "HBV light" model (Seibert, 2002) consists of four routines: snow (not used in this study), soil moisture, response and routing. The model can be run lumped, or semi-distributed. In the latter mode, it is only the soil moisture which can be parameterized in a distributed manner (considering up to three vegetation zones and a selected number of elevation zones) and none of the input data (precipitation, temperature, evaporation) is distributed. Two improvements of the model structure have been made with the development of HBVx. First, an interception volume is introduced, as per the previous section. Second, all of the routines can be run in parameterized and semi-distributed mode, through the designation of two or more separate sub-basins. The basic equations for the linear reservoirs are given in Fig. 3.

The soil routine is based on two parameters: FC (mm), which defines the maximum soil moisture storage or field capacity; this can be emptied by evaporation. β (-) defines the nonlinear function that computes the amount of infiltration water that goes into the runoff generation routine (toRGR) and the amount that stays in the soil routine to fill up the soil moisture storage (SM):

$$\frac{\mathrm{toRGR}}{\mathrm{P}} = \left(\frac{\mathrm{SM}}{\mathrm{FC}}\right)^{\beta} \tag{9}$$

Parameter LP (-) is part of the soil moisture ratio below which the actual sub-catchment evaporation does not reach E_c, due to moisture stress (Seibert, 2002; Uhlenbrook *et al.*, 2004). This reduces the soil evaporation and transpiration value (i.e. net of interception per equation (8) at sub-catchment level) when SM/FC is less than LP.

Only the 2007/08 season data were used, since there were insufficient data points in the 2005/06 season. Initial calibration of the lumped HBV model without interception was carried out to explore the parameter space. The parameter ranges are shown in Table 2, and were selected based on field observations and experience in application of HBV to other catchments.

For the semi-distributed model set-ups, the linear storage coefficients K_0, K_1 and K_2 were higher and the soil storage parameters UZL and FC generally lower for the Gobalidanke sub-catchment. This was done in order to represent the effects of the higher proportion of degraded land in the Gobalidanke sub-catchment (see Fig. 1), from which faster overland and near-surface flows were observed. This field observation is also supported by the typical soil profile in the Gobalidanke sub-catchment: a near-surface clay layer, expected to result in soil storage drying more rapidly.

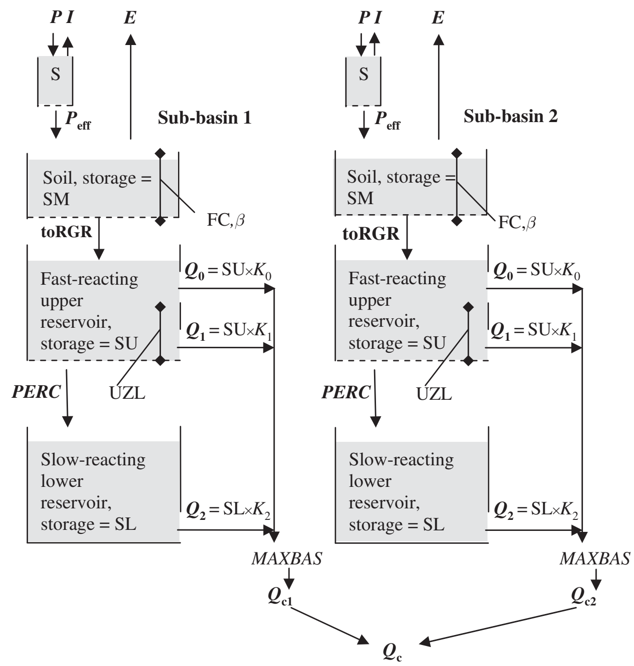

Fig. 3 Schematic diagram of the HBVx model structure in semi-distributed mode with interception routine. Parameters: P = precipitation, S = interception storage (capacity = D), E = soil evaporation and transpiration – see equation (8), I = interception, P_{eff} = effective rainfall, toRGR = moisture transferred to runoff generation routine, UZL = threshold for start of overland flow, PERC = percolation, Q_0 = overland flow, Q_1 = discharge from saturated soil or shallow groundwater, Q_2 = discharge from deep groundwater, Q_c = total discharge from catchment, MAXBAS = routing parameter. All parameters mm d^{-1}, except UZL and FC (mm) and MAXBAS (-). Fluxes are shown in bold and model parameters in italics. Note that, with the exception of Q_c, all fluxes and parameters are different for each of the two sub-catchments.

A stepwise model concept improvement approach (Fenicia *et al.*, 2008) was then used to evaluate the separate and incremental benefits of incorporating the interception routine and of the semi-distributed parameterization. Extensive calibration was carried out manually, supported by 1 000 000 Monte Carlo simulations, within the parameter space selected (Table 2), to: (a) obtain a good fit of the shape of the simulated

Table 2 Parameter ranges for all runs performed in the calibration of HBVx.

Parameter	FC (mm)	β (-)	UZL (mm)	K_0 (d^{-1})	K_1 (d^{-1})	K_2 (d^{-1})	PERC (mm d^{-1})
Minimum	10	1	10	0.25	0.1	0.0001	2
Maximum	150	5	100	1.00	0.7	0.0050	5

Note: MAXBAS was set at 1 and LP at 0.7 throughout all runs. See Fig. 3 for the role of each parameter in the model. No value is given for D as the runs were performed either without interception storage ($D = 0$ mm) or with the single interception storage value derived from multiple regression.

2007/08 rainy season discharge series, and (b) maximize the objective functions. The selected objective functions were the Nash-Sutcliffe coefficient (C_{NS}) and mean volume error (dV_d) (mm year^{-1}):

$$C_{\text{NS}} = 1 - \frac{\sum_{i=1}^{n}\left(Q_{\text{obs},i} - Q_{\text{sim},i}\right)^2}{\sum_{i=1}^{n}\left(Q_{\text{obs},i} - \overline{Q_{\text{obs}}}\right)^2} \quad (10)$$

$$\text{d}V_d = \frac{365 \times \sum_{i=1}^{n}\left(Q_{\text{obs},i} - Q_{\text{sim},i}\right)}{n} \quad (11)$$

where Q_{obs} (mm d^{-1}) is the observed discharge, Q_{sim} (mm d^{-1}) the simulated discharge and n the number of time steps i (days) in the simulation.

For those model set-ups where the interception routine was active, a constant value of D obtained from the multiple linear regression was used, and interception flux I_i was calculated in HBVx, using equation (5). For lumped model set-ups, I_i was calculated at catchment scale for each time step, but for semi-distributed model set-ups it was calculated independently at sub-catchment scale.

A simple sensitivity analysis was carried out for the best parameterization for the eight parameters that were varied during the calibration. The 10% elasticity index (e_{10}) was used as per Cullmann & Wriedt (2008):

$$e_{10} = \frac{\text{Out}_1 - \text{Out}_0}{0.1 \times \text{Out}_0} \quad (12)$$

where Out_0 is the initial model output being studied and Out_1 is the model output after the parameter in question has been increased or decreased by 10% (both were done).

RESULTS

Field data

Rainfall observations showed high spatial and temporal variability, with annual totals for the 2005/06 and 2007/08 seasons close to the long term average annual rainfall at Filabusi, but total rainfall for the 2006/07 season was well below this average (Table 3). The latter observation is probably related to a moderate positive ENSO anomaly which was recorded during that season (Logan *et al.*, 2008).

Examination of the daily rainfall and discharge data from Zhulube for the 2006/07 season (data are only available from February 2007 onwards, when the gauge was operational) does not show a consistent pattern in either the initiation of discharge nor in the source (between the two sub-catchments). The discharge events are highly disconnected, with no observable recession curve (Fig. 4 a). A further factor contributing to the disconnected nature of the discharge events is the tendency for soils observed elsewhere to become hydrophobic during droughts, thus decreasing infiltration (Beven, 2002).

During the 2007/08 season, it can be seen that when there is a difference between the sub-catchment rainfall values, rainfall in the Gobalidanke sub-catchment gives

Table 3 Annual rainfall statistics from field observations in Zhulube catchment, contrasted with the long-term average for Filabusi.

Season	Total annual rainfall (mm year^{-1})	Number of rainy days
2005/06	528	49
2006/07	289	31
2007/08	592	57
Filabusi average, 1921–1996	555	51

Note: For locations see Fig. 1.

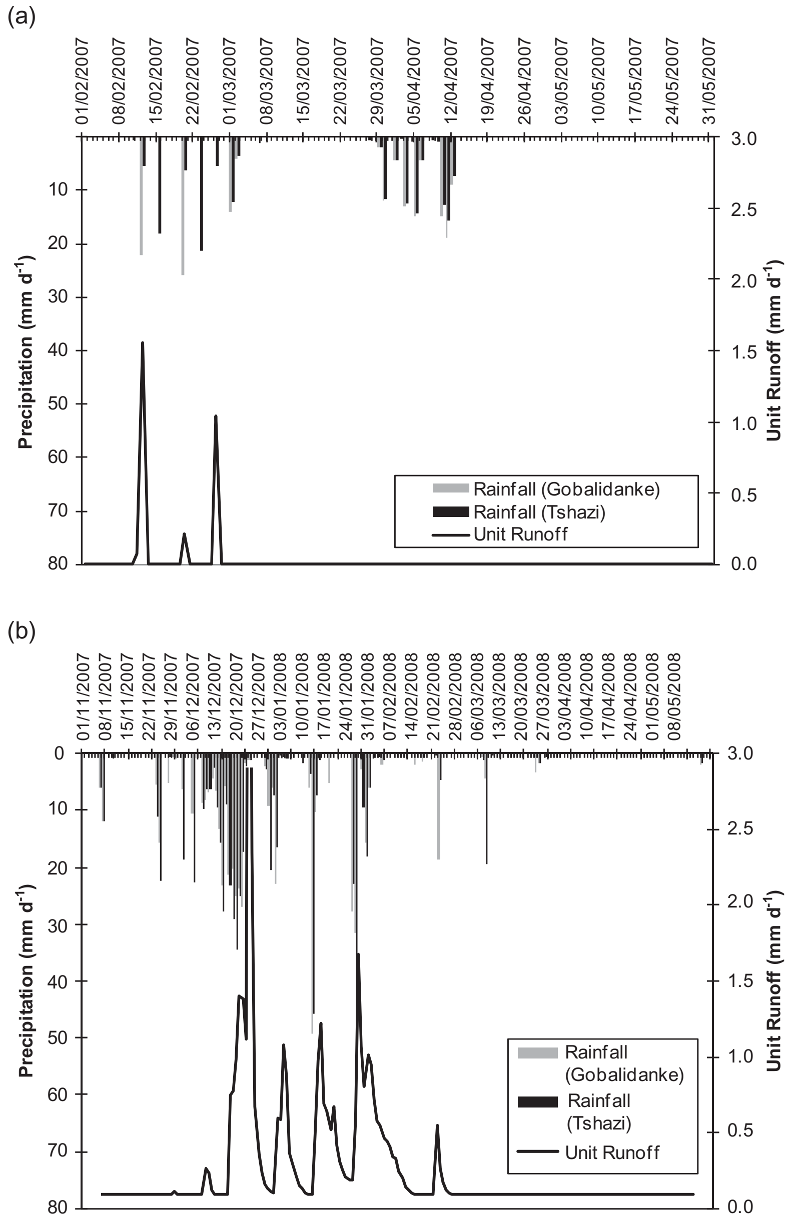

Fig. 4 Observed rainfall, disaggregated by sub-catchments, and discharge, Zhulube catchment: (a) 2006/07 rainy season; and (b) 2007/08 rainy season.

an apparently stronger discharge response than rainfall in the Tshazi sub-catchment: compare for example the discharge recorded on 16.02.2008, in response to 19 mm rainfall in Gobalidanke sub-catchment with the lack of discharge recorded on 01.03.2008 to 20 mm rainfall in Tshazi sub-catchment (Fig. 4b) – despite a higher API of 1.2 mm d^{-1} on the second date, compared to 0.2 mm d^{-1} on the first date. Two peak types can be seen (Table 4): (a) floods lasting less than one week, and (b) flows with recession exceeding two to three weeks. The latter group of floods are associated with much higher antecedent precipitation (Q/API ≥ 1), although the runoff coefficients are variable. If there is any difference in the time of initiation of response, it is not observed and therefore is likely to be at a sub-daily scale (this could also not be observed in the bi-daily raw data). The very sharp recession curves could be caused by (presumed) low antecedent soil moisture and lack of baseflow to this ephemeral river system. This is exacerbated in the Gobalidanke sub-catchment by the shallow soil horizon (above the impermeable clay).

Table 4 Characteristics of flood events recorded in the Zhulube catchment, 2007/08 season.

Date of maximum flow	Total discharge recorded, Q (mm)	Total rainfall recorded, P (mm)	Duration of event (d)	Event runoff coefficient, Q/P	Q/API[a]
04.12.2007	0.33	19.43	2	0.02	0.07
16.12.2007	6.23	131.77	6	0.05	0.16
18.12.2007	10.91	47.69	6	0.23	0.06
29.12.2007	3.66	44.90	19	0.08	0.91
10.01.2008	5.96	60.93	13	0.10	5.47
25.01.2008	9.52	105.71	17	0.09	2.3×10^{-4}

[a]API: antecedent precipitation index.

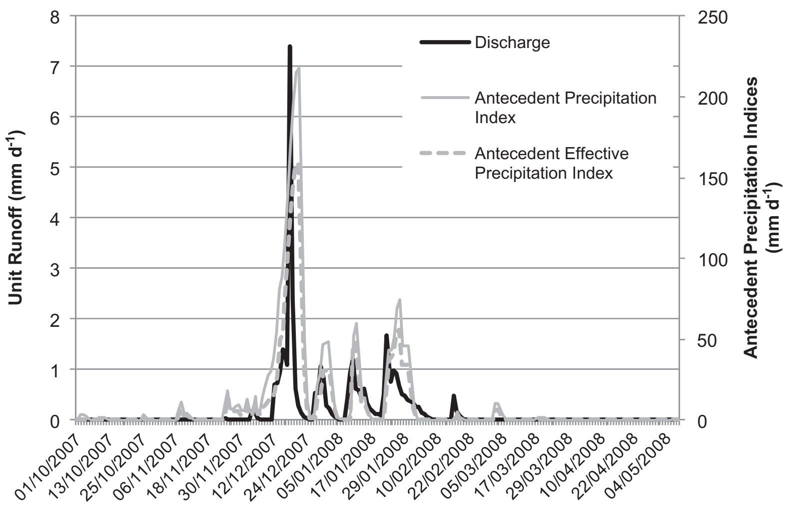

Fig. 5 Discharge compared with the antecedent precipitation indices, as per Equation (1).

Discharge was found to follow the pattern of antecedent precipitation (Fig. 5).

Multiple regression rainfall–runoff model

The results of the model suggest that the consideration of only the previous day's rainfall (as opposed to longer periods of antecedent rainfall) influence the observed discharge (Table 5). Values of between 2 and 6 mm d^{-1} were used for the interception threshold (D); this being the range proposed by De Groen & Savenije (2006). Sensitivity to interception threshold is low, though a threshold of 5 mm d^{-1} gives marginally better results.

Runoff was simulated using an interception threshold of 5 mm d^{-1} (as the threshold giving marginally better correlation; Table 5) and marginally better results were obtained using catchment rainfall, as compared to sub-catchments rainfall (Table 6). The general runoff dynamics were simulated well, except the largest flood of 18.12.2007. Discharge was over-simulated during the start and end of the rainy season (Fig. 6), probably due to the model not considering (soil) storage.

Interception estimations

Given that the results of the multiple regression model favoured a memory of only one day, equation (6) was used as stated above. An interception threshold value of 5 mm d^{-1} was used as before. In the Zhulube catchment, it can be seen that much of the early and late rainfall was intercepted in the 2007/08 season. Interception values decrease slightly on days following heavy rains (Fig. 7). Interception accounted for 56% of rainfall in the 2006/07 season, and 32% of the rainfall in the 2007/08 season. Transpiration and soil evaporation values for the Gobalidanke sub-catchment are (often) lower than for the Tshazi sub-catchment (Fig. 8), due to the minimal forest cover and extensive degraded areas in the former.

Table 5 Correlation coefficients from multiple linear regression of discharge and effective rainfall, Zhulube catchment.

Antecedent rainfall considered in model (days)	Correlation coefficient (-)				
	$D = 2$	$D = 3$	$D = 4$	$D = 5$	$D = 6$
0	0.5797	0.5758	0.5709	0.5652	0.5581
1	0.7087	0.7087	0.7097	0.7098	0.7067
2	0.7452	0.7478	0.7497	0.7507	0.7509
3	0.7599	0.7631	0.7656	0.7674	0.7685
4	0.7600	0.7632	0.7657	0.7675	0.7687
5	0.7778	0.7813	0.7843	0.7868	0.7888
6	0.7788	0.7824	0.7854	0.7881	0.7902
7	0.7788	0.7825	0.7855	0.7881	0.7902

Note: D = interception threshold (mm d^{-1}).

Table 6 Comparison of observed discharge in the Zhulube catchment with simulated discharge using different rainfall series and an interception threshold of 5 mm d^{-1}.

	Observed discharge, Q_{obs}	Simulated discharge, Q_{simZ}
Mean (mm d^{-1})	0.21	0.23
Standard deviation (mm d^{-1})	0.65	0.48
Correlation coefficient, R (-)		0.77
Nash-Sutcliffe coefficient, C_{NS} (-)		0.59

Note: Q_{simZ} = discharge simulated using Zhulube catchment rainfall.

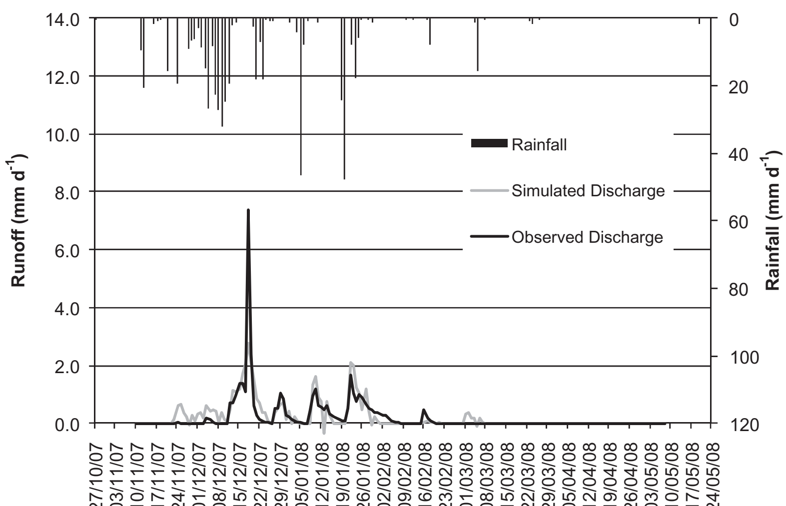

Fig. 6 Observed discharge, Zhulube catchment, compared to that simulated from catchment rainfall using the multiple regression rainfall–runoff model with an interception threshold of 5 mm d^{-1}. Note the over-simulation of discharge during the earliest and latest parts of the season.

HBVx modelling

The automatic calibration of the lumped model set-up without interception storage achieved only relatively low Nash-Sutcliffe coefficients (C_{NS}), and the mean daily volume error (dV_d) values were always below zero (Fig. 9), indicating an over-simulation of the observed discharge. Changing from lumped to semi-distributed mode did not produce any real improvement in the objective functions, with dV_d remaining negative. However, introduction of interception storage did: C_{NS} of 0.503 for the model in semi-distributed

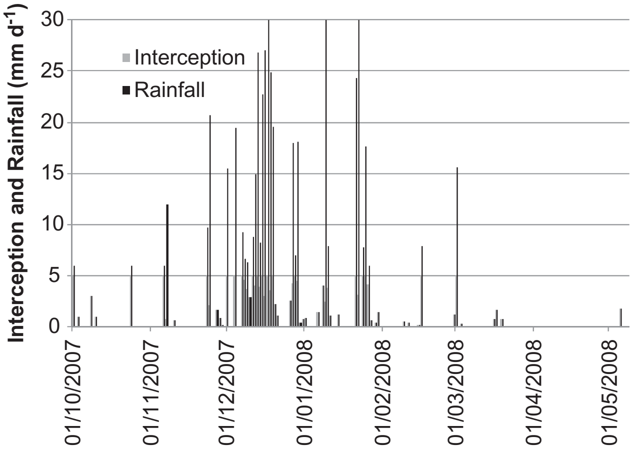

Fig. 7 Daily rainfall and interception, Zhulube catchment, 2007/08 season. Total season rainfall was 592 mm and total season interception was 167 mm. The effect of equation (6) can be seen as interception values decrease slightly on some days following consecutive heavy rains.

mode with interception storage, compared to C_{NS} of 0.290 without (Table 7). The value of dV_d improved from -44.9 mm d^{-1} without interception storage to 6.9 mm d^{-1} with. The semi-distributed set-up with interception storage performed slightly better than the lumped set-up with interception storage. The best parameterization of each model set-up is shown in Table 7 and Fig. 9. Varying the interception threshold D from that determined in the multiple regression consistently produced poorer Nash-Sutcliffe coefficients and mean daily volume errors.

Comparing the two best parameterizations within the semi-distributed model set-up with interception, SI1 and SI2, both have high FC and UZL storage parameters (soil storage and upper groundwater zone storage respectively) and simulate discharge mainly through Q_1 (which should approximate flow from shallow groundwater), with no flow, Q_0 (which should approximate overland flow). Set-up SI1, with slightly lower K_1 value (meaning slower flow, Q_1), gives the best performance in terms of objective functions, although the fit is not so good (see Fig. 9(a)). The model is not able within one parameterization to produce a good fit to both the short, intense discharge peaks (e.g. 18.12.2007) and the slower peaks with developed recessions (e.g. 10.01.2008, 25.01.2008).

It can be seen that the thresholds FC and UZL are not reached in either sub-catchments. Discharge recedes as the upper zone dries out and nearly ceases once the upper zone is dry (compare Fig. 10 (a) and (b), e.g. on 24.12.2007). For the floods which peaked on 10.01.2008 and 25.01.2008, recession over several days is not simulated by the model. The model simulates an extremely small Q_2 flow (which approximates baseflow from deep groundwater); according to field observations this should be zero for most of the year.

The sensitivity analysis (Table 8) showed that the total simulated discharge, Q_1 flow (flow from shallow groundwater, the largest portion of simulated flow) and recharge of the lower groundwater zone are particularly sensitive to PERC (maximum daily flow to lower groundwater zone) and FC, with mean soil moisture

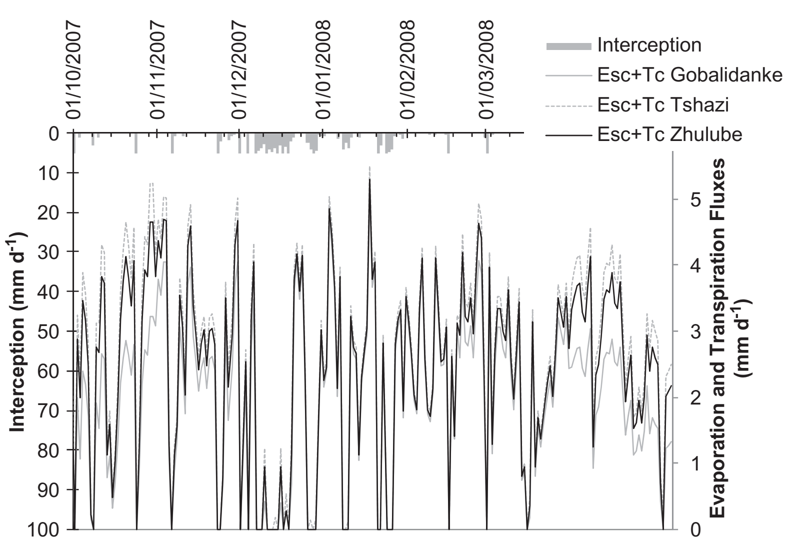

Fig. 8 Computed daily interception and transpiration plus soil evaporation (E_{sc} + T_c), Zhulube catchment, 2007/08. Soil evaporation and transpiration values for the Gobalidanke sub-catchment are generally lower than for the Tshazi sub-catchment.

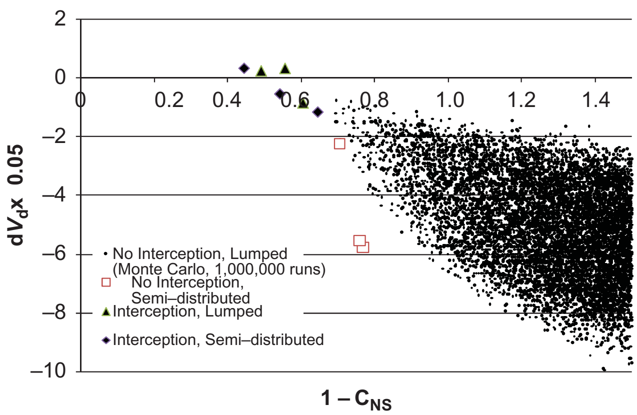

Fig. 9 Scatter-plot of performance of different model set-ups and parameterizations of the HBVx models. The Nash-Sutcliffe coefficient is displayed as $(1 - C_{NS})$ so that both objective functions would be zero for a perfect simulation. The mean daily difference is expressed as $(dV_d \times 0.05)$. For parameterization, see Table 6; for objective functions see equations (10) and (11).

sensitive mainly to FC. After PERC, the model is most sensitive to β, and sensitivity to the hydrological storage coefficients is lower. The model output appears more sensitive to soil and geological parameters. Sensitivity to a decrease in model parameter was generally greater than sensitivity to an increase.

A simple water balance (Table 9) shows the prominent role played by interception. The Tshazi sub-catchment shows greater transpiration and soil evaporation (presumably due to the greater woodland coverage) and less discharge than Gobalidanke sub-catchment.

DISCUSSION

Observed rainfall and discharge characteristics

Observed discharge events were disconnected at catchment level, with short to very short recession curves. This is exacerbated by the high spatial variability in rainfall. In the Tshazi sub-catchment, the disconnected flows are probably caused by the shallow soils which dry out rapidly, resulting in little baseflow and reduced connectivity between events (Farmer *et al.*, 2003). In the Gobalidanke sub-catchment, the presence of an impermeable clay layer limits percolation and thus baseflow. In common with other studies in Zimbabwe (e.g. Bullock, 1992; Bullock & McCartney, 1995; McCartney, 2000) and Zambia (Von der Hayden & New, 2003), the presence of a dambo in Gobalidanke is likely to contribute to discontinuous discharge during the rainy season, as water is retained and transpired by the wetland. There is also no extension of discharge into the dry season, again as seen in studies elsewhere in Zimbabwe. Even after a good season, discharge drops to zero very quickly after a flood event.

Table 7 Parameterization of the HBVx model set-ups which performed best in terms of the selected objective functions during manual calibration.

Set-up	D (mm)	K_0 (d^{-1})	K_1 (d^{-1})	K_2 (d^{-1})	PERC (mm d^{-1})	UZL (mm)	LP (-)	FC (mm)	β (-)	C_{NS} (-)	dV_d (mm d^{-1})
Manual calibration, lumped											
LI1	5	1.00	0.35	0.0005	3	84	0.7	100	4	0.509	4.9
LI2	5	1.00	0.21	0.0005	2	84	0.7	120	4	0.444	6.6
LI3	5	1.00	0.20	0.0030	3	60	0.7	90	4	0.395	−17.0
Manual calibration, semi-distributed											
S1: Gobalidanke	0	0.40	0.30	0.0010	5	30	0.7	35	1	0.231	−115.0
S1: Tshazi	0	0.60	0.15	0.0005	5	40	0.7	50	4		
S2: Gobalidanke	0	1.00	0.15	0.0005	2	50	0.7	80	1	0.242	−110.9
S2: Tshazi	0	1.00	0.20	0.0005	2	60	0.7	90	4		
S3: Gobalidanke	0	1.00	0.30	0.0010	2	60	0.7	100	1	0.296	−44.9
S3: Tshazi	0	1.00	0.21	0.0005	2	84	0.7	140	4		
SI1: Gobalidanke	5	1.00	0.30	0.0010	2	60	0.7	100	1	0.556	6.9
SI1: Tshazi	5	1.00	0.21	0.0005	2	84	0.7	140	4		
SI2: Gobalidanke	5	1.00	0.50	0.0010	2	60	0.7	100	1	0.459	−10.9
SI2: Tshazi	5	1.00	0.35	0.0005	2	84	0.7	140	4		
SI3: Gobalidanke	5	1.00	0.16	0.0015	2	50	0.7	80	1	0.356	−23.5
SI3: Tshazi	5	1.00	0.20	0.0030	2	60	0.7	90	4		

Note: MAXBAS was set at 1 for all set-ups, due the small catchment size. All parameterizations were within the parameter space of the automatic calibration (Table 2). See Fig. 2 for the role of each parameter in the model; for objective functions see equations (10) and (11).

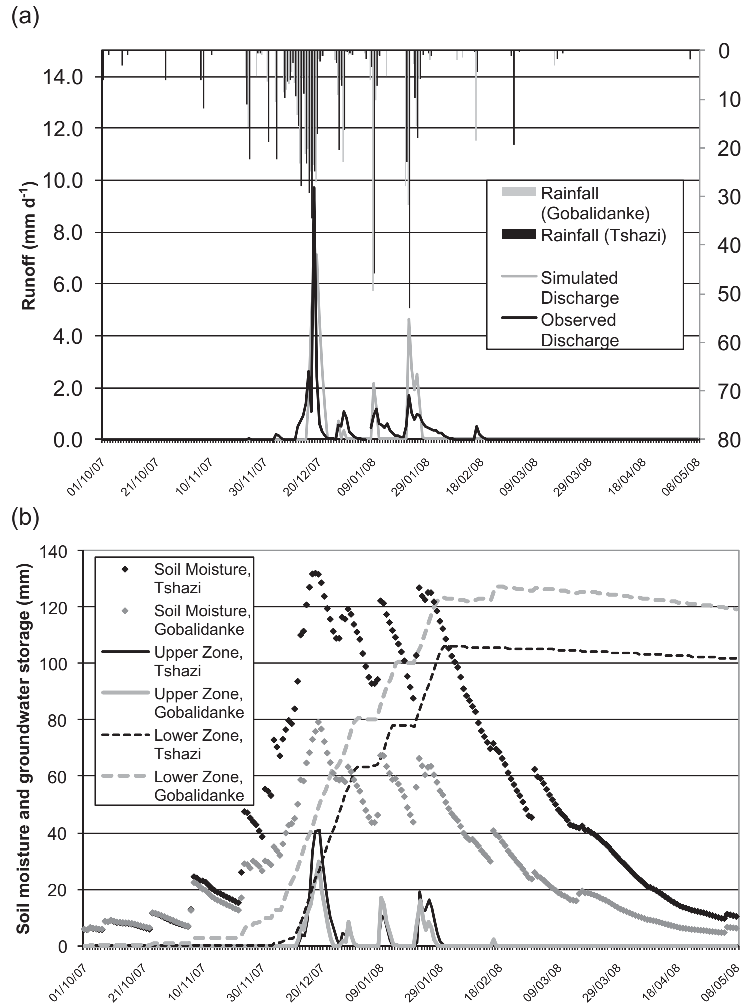

Fig. 10 Model outputs for set-up SI1, which had the best objective function values: (a) observed and simulated discharge and rainfall; and (b) simulated soil moisture and groundwater storage for the two sub-catchments.

Table 8 Local sensitivities of model outputs to model parameters, set-up SI1, calculated using equation (12).

Model output	Elasticity index (e_{10})[a]						
	K_0	K_1	K_2	PERC	UZL	FC	β
Total Q_{sim}	0.000	0.401	0.119	0.818	0.000	1.802	0.456
	0.000	0.423	0.118	0.606	0.000	1.490	0.292
Total Q_1	0.000	0.258	0.000	0.663	0.000	0.595	0.125
	0.000	0.294	0.000	0.570	0.000	0.574	0.098
Recharge	0.000	0.233	0.082	0.594	0.000	0.101	0.231
	0.000	0.266	0.081	0.510	0.000	0.122	0.195
Mean soil moisture	0.000	0.000	0.000	0.000	0.000	1.175	0.169
	0.000	0.000	0.000	0.000	0.000	1.193	0.143

Note: Since set-up SI1 did not produce any overland flow (Q_0), no sensitivity could be calculated for this output. Parameters UZL and FC are both storage threshold parameters and only one of them can be a limiting factor at a time.
[a]The first figure given is for 10% decrease in the model parameter; the second figure for 10% increase.

Table 9 Water balance of the two sub-catchments, based upon model set-up SI1.

Sub-catchment	Rainfall (mm year^{-1})	Interception (mm year^{-1})	Transpiration and soil evaporation (mm year^{-1})	Discharge (mm year^{-1})	Change in soil and aquifer storage (mm year^{-1})
Gobalidanke	506	173	167	70	120
Tshazi	575	164	254	53	206

Flow events were either short, intense peaks lasting less than one week or flows with slower recession, lasting two to three weeks. Variation in flow processes across a rainy season has been shown in many sites in Sub-Saharan Africa (Dubrueil, 1985). The difference in the type of flood in the study site can be associated with differences in antecedent precipitation (Table 4) and could be related to two factors: (a) rainfall intensity (which was not measured), with more intense storms producing the flash floods; and (b) change in soil conditions over the course of the rainy season. For example soil crusting, the formation of thin dense near-surface layer of low hydraulic conductivity, typically occurs before or at the start of the rainy season (Hopmans *et al.*, 2007) or during vegetative droughts (Beven, 2002); the 2006/07 season was a drought. Crusting would decrease infiltration and could lead to flash floods, especially at the beginning of the rainy season. Such behaviour is consistent with Hortonian (infiltration excess) stormflow. Floods later in the season, such as those in late January which were generated mainly in the Gobalidanke sub-catchment, are consistent with saturation overland flow from a dambo (McCartney *et al.*, 1998). Variation in soil parameters such as infiltration rate across a rainy season has been shown at two sites in the Zhulube catchment by Ngwenya (2006): An ungrazed study site showed a change from an initial sorptivity (capillarity) control on infiltration rate to hydraulic conductivity control (Table 10).

Quality control of rainfall data showed that adjacent stations gave close results, and no major changes were noted between measurements by different observers. The composite gauge performed well at lower flows (using the V notch), but there was lower reproducibility of observations from the broad crest.

The two years of measurements from Zhulube already provide some insight into the response of this catchment. However, the variation in flood event type during the 2007/08 season, and the great difference between that season and 2006/07 show that constraining predictive uncertainties may be more complex in highly variable semi-arid catchments than the simpler case of perennial humid catchments (Seibert & Beven, 2009). Understanding of catchment dynamics would have been improved by gauging the two sub-catchments. However, there were no suitable sites upstream of the confluence of the Tshazi and Gobalidanke streams. For future research, the findings of this study would be improved if supported by detailed measurement of soil moisture and groundwater levels. The experimental design included recording rainfall and discharge at sub-hourly time steps. However, such results are not available due to equipment failure and theft.

Modelling results

The HBVx simulation satisfactorily showed the ephemeral, disconnected nature of the flows. The importance of incorporating interception into rainfall–runoff modelling is demonstrated by the substantial improvement in objective function values obtained when this was done in the model – exceeding the gains made by changing from lumped to semi-distributed mode (Fig. 8). The relatively low Nash-Sutcliffe coefficients can be explained by the model failing to simulate the two different observed flood types differently. Shortcomings of the model include the inability to address temporal variability in soil characteristics and the exclusion of some storages which may sustain flow, such as bank and wetland storage. However, the experimental data is insufficient to support a more complex model set-up, with additional storages and fluxes.

The best HBVx simulation (SI1) suggests discharge driven mainly by flow from the fast-reacting upper reservoir (SU), similar to saturation excess overland flow, as expected in the Gobalidanke sub-catchment but not the Tshazi sub-catchment. It simulates the subsurface flow in a physically realistic manner, although there are no field data to compare the simulation with. The model suggests episodic groundwater recharge – see the increase in lower zone groundwater storage in Fig. 9(b) – as reported by Butterworth *et al.* (1999). The estimated groundwater recharge of 100 mm year^{-1} is within the range reported from elsewhere in Zimbabwe by Larsen *et al.* (2002), but somewhat higher than those reported by Farquharson &

Table 10 Field measurements of infiltration rate taken from two sites in the study catchment during the 2005/06 rainy season, using a tension infiltrometer.

Date	Treatment	R^2 (cumulative infiltration: time)	R^2 (cumulative infiltration: time$^{0.5}$)	Conclusion
13.12.2005	Clay fenced	0.999	0.977	Sorptivity
	Clay grazed	0.991	0.997	Hydraulic conductivity
13.01.2006	Clay fenced	0.986	0.997	Hydraulic conductivity
	Clay grazed	0.993	0.994	Hydraulic conductivity
23.01.2006	Clay fenced	0.978	0.998	Hydraulic conductivity
	Clay grazed	0.994	0.993	Sorptivity?
28.01.2006	Clay fenced	0.989	0.996	Hydraulic conductivity
	Clay grazed	0.995	0.994	Sorptivity?
05.02.2006	Clay fenced	0.983	0.997	Hydraulic conductivity
	Clay grazed	0.999	0.981	Sorptivity?
10.02.2006	Clay fenced	0.977	0.999	Hydraulic conductivity
	Clay grazed	0.995	0.990	Sorptivity?
15.02.2006	Clay fenced	0.984	0.997	Hydraulic conductivity
	Clay grazed	0.986	0.996	Hydraulic conductivity
27.02.2006	Clay fenced	0.997	0.985	Sorptivity
	Clay grazed	0.993	0.941	Sorptivity
27.03.2006	Clay fenced	0.999	0.981	Sorptivity
	Clay grazed	0.988	0.993	Sorptivity
13.01.2006	Clay-loam fenced	0.988	0.999	Hydraulic conductivity
	Clay-loam grazed	0.983	0.994	Hydraulic conductivity
23.01.2006	Clay-loam fenced	0.983	0.985	Hydraulic conductivity
	Clay-loam grazed	0.997	0.989	Sorptivity
28.01.2006	Clay-loam fenced	0.978	1.00	Hydraulic conductivity
	Clay-loam grazed	0.891	0.992	Hydraulic conductivity
05.02.2006	Clay-loam fenced	0.997	0.992	Sorptivity?
	Clay-loam grazed	0.359	0.358	Sorptivity?
10.02.2006		Not measured		
15.02.2006	Clay-loam fenced	0.984	0.998	Hydraulic conductivity
	Clay-loam grazed	0.999	0.986	Sorptivity?
27.02.2006	Clay-loam fenced	0.985	0.997	Hydraulic conductivity
	Clay-loam grazed	0.998	0.982	Sorptivity?
27.03.2006	Clay-loam fenced	0.993	0.992	Hydraulic conductivity
	Clay-loam grazed	0.998	0.972	Sorptivity?

Source: Data from study of Ngwenya (2006).

Bullock (1992), Sibanda *et al.* (2009) or Wright (1992). However, it should be remembered that the modelled season (2007/08) had higher than average rainfall (see Table 3).

CONCLUSIONS

The Zhulube catchment has shown strong spatial variability in rainfall, and ephemeral, disconnected discharge events, even in a season with above-average rainfall. Two different flood types were observed, probably caused by different runoff generation processes, influenced by catchment antecedent soil moisture.

The extended HBVx model can satisfactorily model the ephemeral flow, and the minimal baseflow from deep groundwater, but does not appear to perform as well when catchment parameters or processes vary during the duration of a calibration interval. The best HBVx simulation that is supported by field observations in the Gobalidanke sub-catchment suggested that discharge was driven mainly by flow similar to saturation excess overland flow. Hortonian overland flow, as interpreted from field observations in the Tshazi sub-catchment, was not simulated well.

Interception is an important process in the water balance of this semi-arid catchment, accounting for 32% of rainfall in the 2007/08 season but as much as 56% in the drier 2006/07 season. The importance of interception is reflected in significantly improved performance of HBVx once this routine is introduced.

For the future, understanding of Zhulube, and ephemeral, semi-arid catchments of this type, could be improved by a longer time series, and observations at higher temporal resolution. This would allow for a more complex model set-up and the evaluation of the variation of soil parameters in space and time.

Acknowledgements This paper is an output of the CGIAR Challenge Program on Water and Food Project "Integrated Water Resource Management for Improved Rural Livelihoods: Managing risk, mitigating drought and improving water productivity in the water scarce Limpopo basin", led by WaterNet, with additional funding provided by the International Foundation for Science (Grant W4029-1). The opinions and results presented in this paper are those of the authors and do not necessarily represent the donors or participating institutions. Reference rainfall data (from outside the field study sites) were kindly provided by the Department of Meteorological Services, Zimbabwe Ministry of Environment and Tourism. Jan Seibert kindly provided the HBV light 2 code. The assistance of Charles Sakahuni, Baba Mpofu, field assistants Siphatisiwe and Siphetokhule Ncube, Lewis Ndlovu and Sanelisiwe Sibanda, and the District Administrator and Rural District Council of Insiza has been essential and is gratefully acknowledged.

REFERENCES

Allen, R. G., Pereira, L. S., Raes, D. & Smith, M. (1998) Crop evapotranspiration – Guidelines for computing crop water requirements. *FAO Irrigation and Drainage Paper 56*. Rome: FAO.

Beven, K. (2002) Runoff generation in semi-arid areas. In: *Dryland Rivers: Hydrology and Geomorphology of Semi-Arid Channels* (ed. by L. J. Bull & M. J. Kirkby), 57–106. Chichester: Wiley.

Blöschl, G. & Sivapalan, M. (1995) Scale issues in hydrological modelling: a review. *Hydrol. Processes* **9**, 251–290.

Bullock, A. (1992) The role of dambos in determining river flow regimes in Zimbabwe. *J. Hydrol.* **134**, 349–372.

Bullock, A. & McCartney, M. P. (1995) Wetland and river flow interactions in Zimbabwe. In: *L'hydrologie tropicale: géoscience et outil pour le développement* (Actes de la conférence de Paris, Mai 1995) (ed. by P. Chevallier & B. Pouyaud), 305–321. IAHS Publ. 238. Wallingford: IAHS Press.

Butterworth, J. A., MacDonald, D. M. J., Bromley, J., Simmonds, L. P., Lovell, C. J. & Mugabe, F. (1999) Hydrological processes and water resources management in a dryland environment III: groundwater recharge and recession in a shallow weathered aquifer. *Hydrol. Earth System Sci.* **3**, 345–352.

Casenave, A. & Valentin, C. (1992) A runoff capability classification system based on surface features criteria in semi-arid areas of West Africa. *J. Hydrol.* **130**, 231–249.

Chesson, P., Gebauer, R. L. E., Schwinning, S., Huntly, N., Wiegand, K., Ernest, M. S. K., Sher, A., Novoplansky, A. & Weltzin, J. F. (2004) Resource pulses, species interactions, and diversity maintenance in arid and semi-arid environments. *Oecologia* **141**, 236–253.

Cullmann, J. & Wriedt, G. (2008) Joint application of event-based calibration and dynamic identifiability analysis in rainfall–runoff modelling: implications for model parametrisation. *J. Hydroinf.* **10**, 301–316.

De Groen, M. M. & Savenije, H. H. G. (2006) A monthly interception equation based on the statistical characteristics of daily rainfall. *Water Resour. Res.* **42**, W12417. doi:10.1029/2006WR005013.

Didszun, J. & Uhlenbrook, S. (2008) Scaling of dominant runoff generation processes: nested catchments approach using multiple tracers. *Water Resour. Res.* **44**, W02410. doi:10.1029/2006WR005242.

Dubrueil, P. L. (1985) Review of field observations of runoff generation in the tropics. *J. Hydrol.* **80**, 237–264.

FAO (Food and Agriculture Organization) (2010) *Crop Water Information: Maize* [online]. Available from: http://www.fao.org/nr/water/cropinfo_maize.html [Accessed 23 February 2010].

Falkenmark, M., Finlayson, C. M. & Gordon, L. J. (2007) Agriculture, water and ecosystems: avoiding the costs of going too far. In: *Water for Food, Water for Life: A Comprehensive Assessment of Water Management in Agriculture* (ed. by D. Molden), London: Earthscan and Colombo, Sri Lanka: International Water Management Institute.

Farmer, D., Sivapalan, M. & Jothitjangkoon, C. (2003) Climate, soil and vegetation controls upon the variability of water balance in temeperate and semiarid landscapes: downward approach to water balance analysis. *Water Resour. Res.* **39**, WR000328. doi:10.1029/2001WR000328.

Farquharson, F. A. K. & Bullock, A. (1992) The hydrology of basement complex regions of Africa with particular reference to southern Africa. *Geol. Soc. Lond. Spec. Publ.* **66**, 59–76.

Fenicia, F., Savenije, H. H. G., Matgen, P. & Pfister, L. (2008) Understanding catchment behavior through stepwise model concept improvement. *Water Resour. Res.* **44**, WR005563. doi:10.1029/2006WR005563.

Hopmans, J. W., Parlange, J.-V. & Assouline, S. (2007) Infiltration. In: *The Handbook of Groundwater Engineering* (ed. by J. W. Delleur), 7-1–7-18. New York: Taylor and Francis.

Jewitt, G. P. W. (1992) *Process studies for simulation modelling of forest hydrological impacts*. MSc Dissertation (unpublished). Dept Agric. Engng, University of Natal, Pietermaritzburg, South Africa.

Lange, J. & Leinbundgut, C. (2003) Surface runoff and sediment dynamics in arid and semi-arid regions. In: *Understanding Water in a Dry Environment: Hydrological Processes in Arid and Semi-arid Zones* (ed. by I. Simmers), 238, 114–150. International Contributions to Hydrogeology, Rotterdam: Balkema.

Larsen, F., Owen, R., Dahlin, T., Mangeya, P. & Barmen, G. (2002) A preliminary analysis of the groundwater recharge to the Karoo formations, mid-Zambezi basin, Zimbabwe. *Phys. Chem. Earth* **27**, 765–772.

Lidén, R. & Harlin, J. (2000) Analysis of conceptual rainfall–runoff modelling performance in different climates. *J. Hydrol.* **238**, 231–247.

Logan, J. A., Megretskaia, I., Nassar, R., Murray, L. T., Zhang, L., Bowman, K. W., Worden, H. M. & Luo, M. (2008) Effects of the 2006 El Niño on tropospheric composition as revealed by data from the Tropospheric Emission Spectrometer (TES). *Geophys. Res. Lett.* **35**, L03816. doi:10.1029/2007GL031698.

Love, D., Twomlow, S., Mupangwa, W., van der Zaag, P. & Gumbo, B. (2006) Implementing the millennium development food security goals – challenges of the southern African context. *Phys. Chem. Earth* **31**, 731–737.

Love, D., Uhlenbrook, S., Twomlow, S., & van der Zaag, P. (2010) Changing hydroclimatic and discharge patterns in the northern Limpopo basin, Zimbabwe. *Water SA* **36**, 335–350.

Makarau, A. & Jury, M. R. (1997) Predictability of Zimbabwe summer rainfall. *Int. J. Climatol.* **17**, 1421–1432.

Martinez-Mena, M., Castillo, V. & Albaladejo, J. (1998) Hydrological and erosional response to natural rainfall in a semi-arid area of south-east Spain. *Hydrol. Processes* **15**, 557–571.

Masih, I., Uhlenbrook, S., Maskey, S., Ahmad, M. D. & Islam, M. D. A. (2008) Estimating ungauged stream flows based on model regionalization – examples from the mountainous, semi-arid Karkheh river basin, Iran. In: *Predictions for Hydrology, Ecology, and Water Resources Management: Using Data and Models to Benefit Society* (ed. by J. Brhuthans, K. Kovar, & Z. Hrkal), (Proc. HydroPredict 2008 Conf., Prague, Czech Republic, 15–18 September 2008) IAHS Press, Wallingford, UK.

McCartney, M. (2000) The water budget of a headwater catchment containing a dambo. *Phys. Chem. Earth B* **25**, 611–616.

McCartney, M., Butterworth, J., Moriarty, P. & Owen, R. J. S. (1998) Comparison of the hydrology of two contrasting headwater catchments in Zimbabwe. In: *Hydrology, Water Resources and Ecology in Headwaters*, (ed. by K. Kovar, U. Tappeiner, N. E. Peters, & R. G. Craig), (Proc. Headwaters'98 Conf., Merano, Italy, 20–23 April 1998), 515–522. IAHS Publ. 248. Wallingford, IAHS Press.

Mugabe, F. T., Hodnett, M. & Senzanje, A. (2007) Comparative hydrological behaviour of two small catchments in semi-arid Zimbabwe. *J. Arid Environ.* **69**, 599–616.

Ngwenya, P. T. (2006) Effect of soil degradation from grazing pressure on rangeland soil hydrology. MSc Dissertation (unpublished), Integrated Water Resources Management Programme, University of Zimbabwe.

Nyabeze, W. R. (2004) Estimating and interpreting hydrological drought indices using a selected catchment in Zimbabwe. *Phys. Chem. Earth* **29**, 1173–1180.

Oudin, L., Hervieu, F., Michel, C., Perrin, C., Andréassian, V., Anctil, F. & Loumagne, C. (2005) Which potential evapotranspiration input for a lumped rainfall–runoff model? Part 2: Towards a simple and efficient potential evapotranspiration model for rainfall–runoff modelling. *J. Hydrol.* **303**, 290–306.

Savenije, H. H. G. (2004) The importance of interception and why we should delete the term evapotranspiration from our vocabulary. *Hydrol. Processes* **18**, 1507–1511.

Schulze, R. E. & Hohls, B. C. (1993) A generic hydrological land cover and land use classification with decision support systems for use in models. In: *Proc. 6th South African National Hydrology Symposium*, University of Natal, Pietermaritzburg, Department of Agricultural Engineering, 547–555.

Schulze, R. E., Lechler, N. L., & Hohls, B. C. (1995) Land cover and treatment. In: *The ACRU Theory Manual, Hydrology and Agrohydrology* (ed. by R. E. Schulze). South Africa: School of Bioresources Engineering and Environmental Hydrology, University of KwaZulu-Natal. Available from: http://www.ukzn.ac.za/unp/beeh/acru/documentation/theory/AT_chapter6.PDF [Accessed 27 February 2010].

Seibert, J. (1999) Regionalisation of parameters for a conceptual rainfall–runoff model. *Agric. For. Met.* **98–99**, 279–293.

Seibert, J. (2002) *HBV Light Version 2 User's Manual*. Sweden: Environmental Assessment Department, SLU.

Seibert, J. & Beven, K. J. (2009) Gauging the ungauged basin: how many discharge measurements are needed? *Hydrol. Earth System Sci.* **13**, 883–892.

Seyam, I., Savenije, H. H. G., Aerts, J. & Schepel, M. (2000) Algorithms for water resources distribution in international river basins. *Phys. Chem. Earth B* **25**, 309–314.

Sibanda, T., Nonner, J. C. & Uhlenbrook, S. (2009) Comparison of groundwater recharge estimation methods for the semi-arid Nyamandhlovu area, Zimbabwe. *Hydrogeol. J.* **17**, 1427–1441.

Sivakumar, M. Y. K., Das, H. P. & Brunini, O. (2005) Impact of present and future climate variability and change on agriculture and forestry in the arid and semi-arid tropics. In: *Increasing Climate Variability and Change: Reducing the Vulnerability of Agriculture and Forestry* (ed. by J. Salinger, M.Y. K. Sivakumar, & R. P. Motha), 31–72. Dordrecht: Springer.

Sivapalan, M., Takeuchi, K., Franks, S. W., Gupta, V. K., Karambiri, H., Lakshmi, V., Liang, X., McDonnell, J. J., Mendiondo, E. M., O'Connell, P. E., Oki, T., Pomeroy, J. W., Schertzer, D., Uhlenbrook, S. & Zehe, E. (2003) IAHS Decade on Predictions in Ungauged basins (PUB), 2003–2012: Shaping an exciting future for the hydrological sciences. *Hydrol. Sci. J.* **48**(6), 857–880.

Smith, G. N. & Rethman, N. F. G. (2000) The influence of tree thinning on the soil water in a semi-arid savanna of southern Africa. *J. Arid Environ.* **44**, 41–59.

Tsiko, T. C., Makurira, H., Gerrits, A. M. J. & Savenije, H. H. G. (2008) Measuring forest floor and canopy interception in a savannah ecosystem (a case study of Harare, Zimbabwe). In: *Abstract Volume, 9th WaterNet/WARFSA/GWP-SA Symp.,* November 2008, Johannesburg, South Africa, 9. Available from: http://www.waternetonline.ihe.nl/symposium/9/full%20papers/hy/Tsiko,%20T.pdf [Accessed 23 February 2010].

Tunhuma, N., Kelderman, P., Love, D. & Uhlenbrook, S. (2007) Environmental impact assessment of small scale resource exploitation: the case of gold panning in Zhulube catchment, Limpopo basin, Zimbabwe. In: *Abstract volume, 8th WaterNet/WARFSA/GWP-SA Symp.* [online], November 2007. Livingstone, Zambia, 47. Available from: http://www.bscw.ihe.nl/pub/bscw.cgi/d2607085/Tunhuma1.pdf [Accessed 23 February 2010].

Uhlenbrook, S., Roser, S. & Tilch, N. (2004) Hydrological process representation at the meso-scale: the potential of a distributed, conceptual catchment model. *J. Hydrol.* **291**, 278–296.

Unganai, L. S. & Mason, S. J. (2002) Long-range predictability of Zimbabwe summer rainfall. *Int. J. Climatol.* **22**, 1091–1103.

Von der Hayden, C. J. & New, M. G. (2003) The role of a dambo in the hydrology of a catchment and the river network downstream. *Hydrol. Earth System Sci.* **7**, 339–357.

Wright, E. P. (1992) The hydrogeology of crystalline basement aquifers in Africa. *Geol. Soc. Lond. Spec. Publ.* **66**, 1–27.